(Preprint) AAS 11-452

ABORT OPTIONS FOR HUMAN MISSIONS TO EARTH-MOON HALO ORBITS

Mark Jesick*

Abort trajectories are optimized for human halo orbit missions about the translunar libration point (L_2), with an emphasis on the use of free return trajectories. Optimal transfers from outbound free returns to L_2 halo orbits are numerically optimized in the four-body ephemeris model. Circumlunar free returns are used for direct transfers, and cislunar free returns are used in combination with lunar gravity assists to reduce propulsive requirements. Trends in orbit insertion cost and flight time are documented across the southern L_2 halo family as a function of halo orbit position and free return flight time. It is determined that the maximum amplitude southern halo incurs the lowest orbit insertion cost for direct transfers but the maximum cost for lunar gravity assist transfers. The minimum amplitude halo is the most expensive destination for direct transfers but the least expensive for lunar gravity assist transfers. The on-orbit abort costs for three halos are computed as a function of abort time and return time. Finally, an architecture analysis is performed to determine launch and on-orbit vehicle requirements for halo orbit missions.

INTRODUCTION

One strategy for developing human exploration capability beyond low-Earth orbit (LEO) involves missions to destinations progressively farther from Earth to establish the technologies and confidence necessary for trips through heliocentric space and ultimately to Mars.[1] Crewed missions to such intermediate destinations provide operational experience in dealing with solar and cosmic radiation, developing life support systems longevity, and measuring psychological and psychosocial effects of long-duration spaceflight beyond LEO. Such missions also validate technology for in-space propulsion and habitats to be used for subsequent missions. One possible destination along this path for future human space exploration is a halo orbit in the Earth-moon system. A mission to a halo orbit around the translunar libration point (L_2), for example, would provide experience in spaceflight further from the Earth than ever before while remaining within several days flight time of Earth.

In addition to serving as a location for the demonstration and development of long-duration human spacecraft systems, halo orbits have other advantages for exploration missions. A properly chosen L_2 halo maintains a constant view of Earth and, therefore, can be used as a lunar farside communications relay.[2,3] Since a halo orbit can be maintained for relatively low stationkeeping costs,[4] the halo could also serve as an aggregation orbit for spacecraft infrastructure. A supply station in an aggregation halo would allow a crew vehicle to resupply here before departing for other

*Engineer, Space Concepts Division, Analytical Mechanics Associates, Inc., 303 Butler Farm Rd., Hampton, Virginia 23666.

locations of interest in the Earth-moon system and elsewhere in the solar system, such as near-Earth asteroids and Mars.[5] Further, a crewed spacecraft in an L_2 halo could be used to remotely operate robots on the lunar surface with little lag time. Telerobotic operations reduce propulsive requirements by keeping humans and associated life-support systems in orbit while a smaller robotic vehicle may descend to the surface to perform tasks that are repetitive, dangerous, or that do not require human presence. Another advantage of L_2 halos is the low orbit insertion cost when using an outbound ballistic lunar transfer (BLT).[6,7] Such transfers are not desirable for human missions because of the increased flight time, but BLTs are ideal for cargo transport where flight time may not be a concern.

For human missions to the lunar surface, leaving an orbital vehicle in an L_2 halo has advantages over using a low lunar orbit (LLO) as in the Apollo program. One disadvantage of using an LLO is that, for solar-powered spacecraft, periodic solar eclipses necessitate alternate on-board power systems. Also, LLOs incur unavoidable periods where the spacecraft loses sight of the Earth. Though it was determined that these periodic communication blackouts with the Apollo command module during lunar orbit were not calamitous,[8] it was not permissible to conduct a lunar farside landing without a more dedicated communications relay. In fact, an L_2 relay spacecraft was considered to enable an Apollo 17 farside landing, but the idea was later abandoned.[9] In contrast to the LLO rendezvous mode of Apollo, an L_2 halo orbit rendezvous mode—that retains a vehicle in the halo during surface operations—allows farside landings while maintaining a constant Earth communication relay. An L_2 halo destination can also reduce outbound propulsive requirements by employing a lunar gravity assist (LGA). Such a mission allows continuous communications from Earth departure through Earth return, except possibly for a period of time between the LGA and halo orbit insertion (HOI). And, because the halo is quasi-periodic on the farside of the moon, propulsive costs to lunar surface destinations do not vary significantly over time as they do for a polar LLO, for example.

Before humans travel to a halo orbit, it is prudent to analyze the abort options that enable a safe Earth return for crew. This study analyzes abort trajectories for halo missions during the outbound and on-orbit flight phases. For the outbound leg, a free return strategy is used to provide a ballistic Earth return option. Circumlunar free returns are employed for halo direct injection, and cislunar free returns are used in combination with an outbound LGA to reduce orbit insertion costs. A previously developed tool[10] focused on targeting LLOs is extended to halo orbit destinations. The outbound and on-orbit abort problems are solved with the constrained, sequential quadratic programming algorithm `VF13`* where the sum of the impulsive maneuver magnitudes is minimized. Trajectories are numerically integrated in a four-body model with the Earth, moon, and sun as active gravitating bodies. LGA transfers are also optimized with `VF13` but within the framework of the Copernicus trajectory design and optimization software.[11,12] The free return geometry is chosen by the optimizer to minimize the orbit insertion maneuver while satisfying Earth departure and arrival constraints. Translunar injection (TLI) and HOI costs are analyzed as a function of the halo orbit location and free return flight time. In addition to the work on the use of outbound free returns, an analysis of the direct abort costs from the destination halo orbit to Earth is performed for various halos. Analysis of abort trajectory characteristics performed in this study is used to make recommendations for preferred mission architectures. Some launch vehicle and on-orbit vehicle configurations are considered to determine which combinations enable the missions discussed in this study.

*Description available at `http://www.hsl.rl.ac.uk/archive/specs/vf13.pdf` [accessed 19 December 2012].

DYNAMICS

The primary dynamic environment used in this study is the four-body model in which the spacecraft of negligible mass moves under the gravitational influence of a spherical Earth, moon, and sun. The acceleration of the spacecraft relative to the moon in this model is

$$\ddot{\boldsymbol{r}} = -\frac{\mu_M}{r^3}\boldsymbol{r} - \mu_E\left[\frac{\boldsymbol{r}-\boldsymbol{r}_{ME}}{|\boldsymbol{r}-\boldsymbol{r}_{ME}|^3} + \frac{\boldsymbol{r}_{ME}}{r_{ME}^3}\right] - \mu_S\left[\frac{\boldsymbol{r}-\boldsymbol{r}_{MS}}{|\boldsymbol{r}-\boldsymbol{r}_{MS}|^3} + \frac{\boldsymbol{r}_{MS}}{r_{MS}^3}\right] \tag{1}$$

where $\boldsymbol{r}$ is the position relative to the moon; μ_M, μ_E, and μ_S are the gravitational parameters of the moon, Earth, and sun; and $\boldsymbol{r}_{ME}$ and $\boldsymbol{r}_{MS}$ are the time-varying moon-Earth and moon-sun vectors. The base frame is the J2000 frame where the principal direction points from the Earth to the vernal equinox at the J2000 epoch. The fundamental plane contains the Earth's equator at epoch, and the third axis is positive in the direction of Earth's geographic north pole. Solar system geometry is taken from the planetary and lunar ephemeris DE 421 [13] with the SPICE toolkit. [14]

A rotating-pulsating reference frame is defined in which the principal direction, $\hat{\boldsymbol{x}}(t)$, rotates with the Earth-moon line and points from the Earth to the moon. The $\hat{\boldsymbol{z}}(t)$ axis is normal to the moon's geocentric orbital plane, and $\hat{\boldsymbol{y}}(t) \equiv \hat{\boldsymbol{z}}(t) \times \hat{\boldsymbol{x}}(t)$. The distance unit is scaled by the Earth-moon distance, $r_{EM}(t)$, so the moon's position vector in this frame is $\boldsymbol{r}_M = [1 \quad 0 \quad 0]^\top$. This reference frame is useful in the construction and visualization of free returns and halo orbits in the four-body ephemeris model.

The circular restricted three-body problem (CRTBP) is also discussed in the context of generating halo orbits and lunar free returns. This model assumes a circular lunar orbit at constant angular velocity and negligible spacecraft mass. Under these assumptions, the CRTBP is an autonomous system when modeled with a rotating reference frame; this feature is useful in generating periodic orbits and any symmetric trajectories. The $\hat{\boldsymbol{i}}$ axis of this frame points from the Earth to the moon; the $\hat{\boldsymbol{j}}$ axis points in the direction of the moon's velocity; and $\hat{\boldsymbol{k}} \equiv \hat{\boldsymbol{i}} \times \hat{\boldsymbol{j}}$. Throughout this study, the $\hat{\boldsymbol{i}}\hat{\boldsymbol{k}}$ plane of the CRTBP and the $\hat{\boldsymbol{x}}\hat{\boldsymbol{z}}$ plane of the rotating-pulsating frame in the four-body model are referred to as the "vertical" plane for convenience.

HALO ORBIT TARGETING

Periodic halos are possible in the CRTBP but not in the four-body model due to solar gravity and the moon's non-circular orbit. Though not modeled here, solar radiation pressure, planetary perturbations, higher-order lunar gravity terms, etc. will also perturb the halo from its idealized CRTBP orbit. Therefore, a halo in a more realistic solar system is a quasi-periodic orbit in the rotating-pulsating frame that is geometrically similar to a periodic halo in the CRTBP. A propulsion system must be used to maintain the quasi-periodic halo due to these differences. Since the four body model is a non-autonomous system, unlike the CRTBP in rotating coordinates, an epoch must be specified; each quasi-periodic halo in this study begins at the epoch of 12:00 AM January 1st, 2025.

In the CRTBP, if an orbit contains two perpendicular crossings of the vertical ($\hat{\boldsymbol{i}}\hat{\boldsymbol{k}}$) plane, it is a periodic orbit. A typical method of targeting periodic orbits in the CRTBP begins with an orbit with an orthogonal crossing of the vertical plane and numerically targets a second orthogonal crossing. This method is used in the four-body model to target quasi-periodic halos over one pseudo-period. The initial spacecraft position lies in the vertical plane at a given epoch, and the spacecraft's velocity

is perpendicular to the vertical plane. The free parameters of this targeting scheme are

$$\boldsymbol{x}_p \equiv \begin{bmatrix} \tau & z_0 & \dot{y}_0 \end{bmatrix}^\top_{1\times 3} \tag{2}$$

where τ is the pseudo-period of the orbit, z_0 is the initial $\hat{\boldsymbol{z}}$ coordinate in the rotating-pulsating frame, and $\dot{y}_0$ is the initial $\hat{\boldsymbol{y}}$ velocity in the rotating-pulsating frame. After propagating the trajectory through an elapsed time τ, another perpendicular plane crossing is targeted by requiring the following constraints to be satisfied:

$$\boldsymbol{c} \equiv \begin{bmatrix} y(\tau) \\ \dot{x}(\tau) \\ \dot{z}(\tau) \end{bmatrix}_{3\times 1} = \mathbf{0} \tag{3}$$

Two families of halos exist at each of the collinear libration points. To distinguish between the two, a "northern" halo is defined as an orbit whose maximum amplitude $\hat{\boldsymbol{z}}$ coordinate is above the Earth-moon plane, and a "southern" halo is defined as an orbit whose maximum amplitude $\hat{\boldsymbol{z}}$ coordinate is below the Earth-moon plane. The L_2 southern halo family, denoted L_2s, is investigated in this study; the family is shown in the CRTBP in Figure 1. In Fig. 1(c) and Fig. 1(d), the normalized position of a halo is its maximum $\hat{\boldsymbol{i}}$ coordinate divided by the Earth-moon distance. It is seen that halos near the moon reach nearly 80000 km out of the Earth-moon plane. As the halos move toward L_2, the orbits flatten into the Earth-moon plane, and the orbital period increases from eight days to more than 14.5 days. For more details of halo orbit generation, see Howell,[15] Farquhar,[16] or Breakwell.[17] For a general overview of halo orbits and a history of their discovery and investigation, see Howell.[18]

FREE RETURN TARGETING

A free return orbit is useful for human missions since it is a ballistic Earth return trajectory that can be followed in an abort scenario. If adverse or unforeseen circumstances arise, the spacecraft may remain on the trajectory and return to Earth without a propulsive maneuver. Free returns are generated first in the CRTBP[19] before being transitioned to the four-body model by scaling the CRTBP quantities to the Earth-moon distance at the given epoch. Because of solar gravity and because the moon's orbit about the Earth-moon barycenter is not circular, at iterative procedure is required to satisfy feasibility constraints. The initial free return constructed in the CRTBP is symmetric, but no symmetry requirements remain in the four-body model, even though some trajectories appear symmetric when viewed at the scale of the Earth-moon distance.

A circumlunar free return is a free return which passes around the farside of the moon, and a cislunar free return is one which doesn't circumnavigate the moon when viewed in the rotating-pulsating frame. In other words, the flyby point near the moon in the normalized rotating-pulsating frame is located at $x > 1$ for a circumlunar free return and $x < 1$ for a cislunar free return. Figure 2(a) shows a circumlunar example, and Figure 2(b) shows a cislunar example. One qualitative difference to observe is that, at these lunar flyby altitudes, the cislunar free return reaches a distance nearly twice as far from the Earth-moon line as the circumlunar free return. This makes the cislunar free return's flight time (13.1 days) almost five days greater than the circumlunar free return's flight time (8.3 days). The extended flight time is even more obvious in the non-rotating frame (not shown) where the cislunar free return passes through apogee on its inbound and outbound path whereas the circumlunar free return does not. The Earth departure and return speeds are similar for each type.

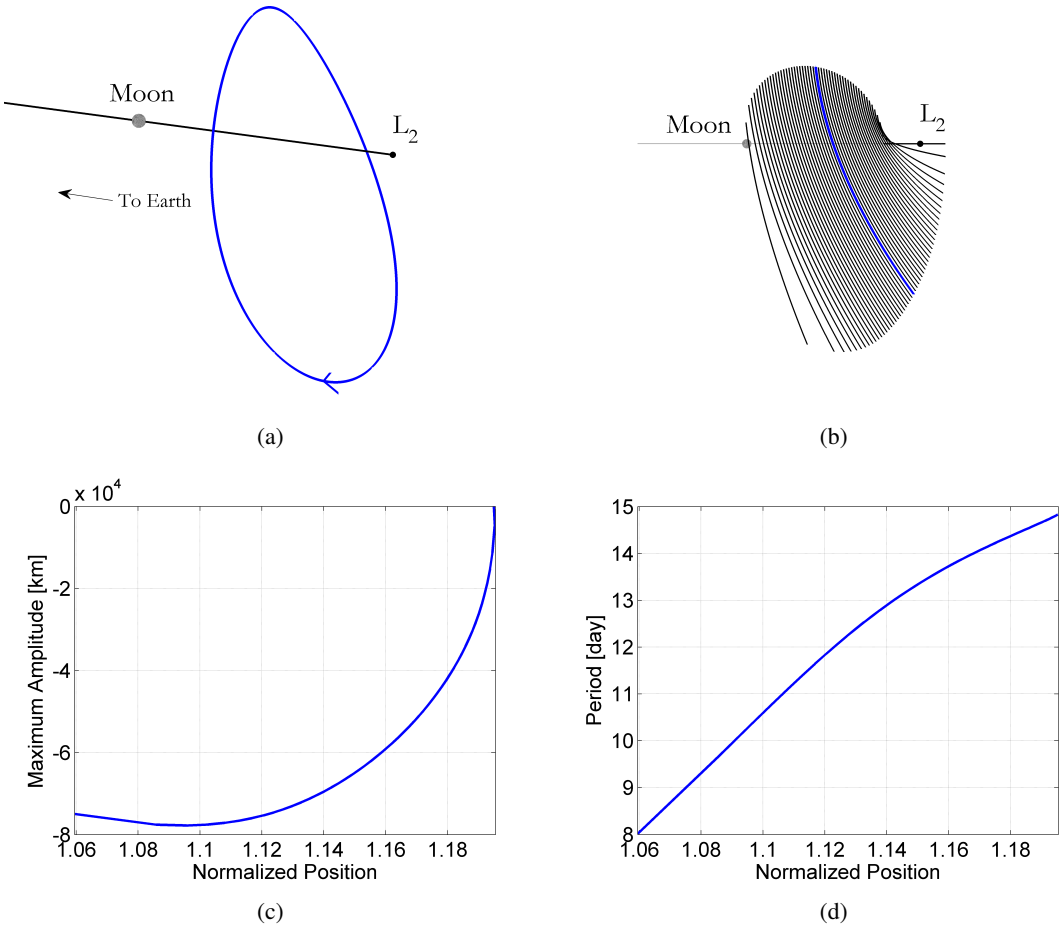

Figure 1. Translunar libration point southern halo family in the CRTBP: a) example halo, b) halo family projection on $\hat{i}\hat{k}$ plane, c) maximum amplitude, and d) orbital period as a function of normalized $\hat{i}$ position.

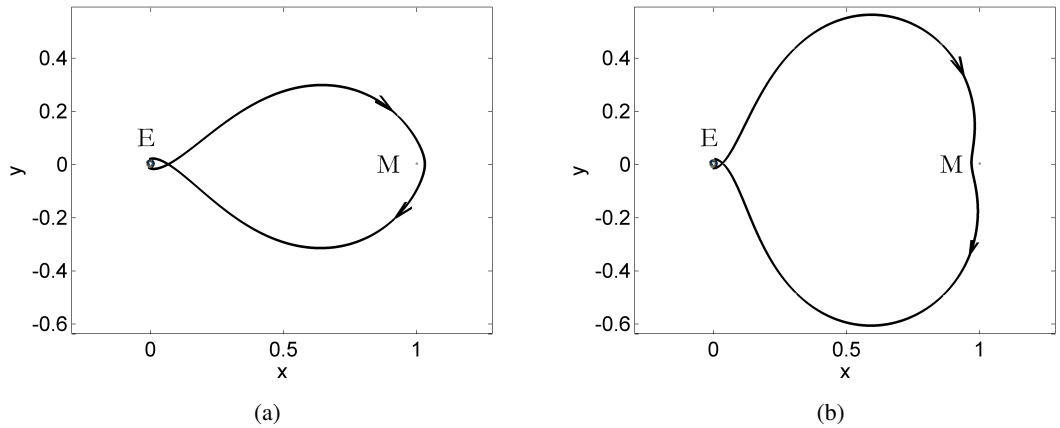

Figure 2. Free returns in the four-body ephemeris model, visualized in the normalized rotating-pulsating frame: a) circumlunar and b) cislunar.

Both cislunar and circumlunar transfers are targeted with the same method. A forward-time segment is propagated from the flyby point to Earth, and a backwards-time segment is propagated from flyby to Earth, targeting an altitude and flight path angle at each point. The flyby point is defined as the point nearer to the moon than the Earth where the spacecraft passes through the vertical plane of the rotating-pulsating frame. The parameters of the free return targeting sub-problem are

$$\boldsymbol{x}_p \equiv \begin{bmatrix} x & z & \boldsymbol{v}^\top \end{bmatrix}^\top_{1\times 5} \tag{4}$$

where x and z are the radial and normal position components of the flyby point in the rotating-pulsating frame, and $\boldsymbol{v}$ is the flyby velocity expressed in the rotating-pulsating frame. The y position at flyby is set to zero; therefore, the free return must pass through the vertical plane. Additional constraints require: the spacecraft to spend a minimum amount of the time on the free return, the round-trip free return flight time to be less than 21 days, and the osculating perilune altitude to be greater than 100 km. Constraints at TLI require

$$\boldsymbol{c} \equiv \begin{bmatrix} h_{TLI} - h^*_{TLI} \\ \gamma_{TLI} - \gamma^*_{TLI} \end{bmatrix}_{2\times 1} = \boldsymbol{0} \tag{5}$$

where h and γ are the altitude and flight path angle, and an asterisk denotes a targeted value. Constraints on the departure inclination and the Earth entry interface (EEI) conditions require

$$\boldsymbol{d} \equiv \begin{bmatrix} f(i_{TLI}) \\ f(h_{EEI}) \\ f(\gamma_{EEI}) \end{bmatrix}_{3\times 1} \geqslant \boldsymbol{0} \tag{6}$$

where i is the inclination and

$$f(x) \equiv (x_{MAX} - x)(x - x_{MIN}) \tag{7}$$

Requiring $f(x) \geqslant 0$ is equivalent to requiring $x_{MIN} \leqslant x \leqslant x_{MAX}$; using $f(x)$ is more efficient in this case because the chosen optimizer requires one-sided inequality constraints. The constraint values used in this study are listed in Table 1.

Table 1. Free return constraint values.

Quantity	Minimum	Maximum	Units
Earth departure altitude	241	241	km
Earth departure flight path angle	0	0	deg
Earth departure inclination	28.5	60	deg
Earth return altitude	120	125	km
Earth return flight path angle	-7	-6	deg
Free return flight time	0	21	day
Free return osculating perilune altitude	100	∞	km

FREE RETURN ABORTS

To reach the targeted halo orbits, two types of outbound transfers are used. A direct transfer uses a circumlunar free return as the initial trajectory in its translunar phase, and an LGA transfer uses a cislunar free return as the initial portion of its translunar trajectory. In each case, a maneuver may be performed to depart the free return to retarget the trajectory for the destination halo to lower

the HOI cost. A maneuver is also applied at the flyby point of LGA transfers. An example direct transfer is shown in Figure 3(a), and an example LGA transfer is shown in Figure 5.

The optimization parameters associated with the free return are identical for both direct and LGA transfers, as outlined in the previous section. Additionally, the time and the three components of each of the HOI maneuver are free parameters. Direct transfers include the retargeting maneuver and the orbit insertion maneuver whereas LGA transfers include these two maneuvers plus the maneuver at lunar flyby. The flyby state is parameterized by its eccentricity, inclination, right ascension, and argument of periapsis with respect to the moon, all of which are optimization variables. The flyby altitude is 100 km. For both direct and LGA transfers, the cost function to be minimized is the sum of the magnitudes of the impulsive maneuvers.

Two example transfers are analyzed for each trajectory type, and the L_2s halo family is scanned to understand trends in the cost and flight time. For the scans, 13 halos are targeted, ranging from near-rectilinear halos near the moon to near-Lyapunov (nearly flat) halos near L_2.

Direct Results

Figure 3(a) shows an optimal direct free return transfer to the $x = 1.2991$ L_2s halo, where the halo's normalized position is its maximum x position divided by the Earth-moon distance. The spacecraft departs Earth on the free return and remains on it for one day before performing an impulsive maneuver to retarget for halo orbit insertion. In this case, the round-trip free return flight time is constrained to be no greater than 10 days (such a constraint would be imposed based on the longevity of onboard life support systems). However, decreasing this time usually increases the propulsive cost of HOI. Therefore, if reducing the spacecraft return time on the free return is a significant objective, it could prove effective to minimize the round-trip free return flight time while bounding the ΔV to the propulsive capability of the vehicle. Figure 3(b) shows a case for the same target halo where the round-trip free return flight time constraint is inactive. It is seen in this figure that the free return's apogee has increased to a point nearly tangent to the halo orbit to minimize the cost function. This gives a savings of over 60 m/s relative to the constrained case. The free return is nearly symmetric about the vertical plane, unlike when the flight time was constrained. The greatest advantage of allowing the free return flight time to vary is that in the optimal solution the retargeting maneuver vanishes, and the spacecraft remains on the circumlunar free return until inserting into the destination halo orbit. In other words, the best transfer (excluding lunar flybys and ballistic lunar transfers) is a free return. The TLI cost and orbit insertion cost are actually cheaper in the constrained case, but the constrained case is more expensive overall because the retargeting maneuver requires almost 100 m/s to boost the spacecraft out to the radius of the target halo. The lone benefit of the constrained case is that the round-trip free return flight time is almost two days less. See Table 2 for a comparison of the constrained (labeled "Direct 1") and the unconstrained (labeled "Direct 2") cases.

Direct transfers are optimized for a range of L_2s halos, varying from near-rectilinear halos near the moon to near-Lyapunov halos near L_2. Some trends in direct transfers are shown in Figure 4; in these examples, the free return flight time constraint is not active. The first subfigure, Figure 4(a), shows the HOI cost and the total cost. The maximum cost proportion due to HOI is approximately 25% of the total over the L_2s family, indicating the overall cost is dominated by the TLI maneuver. However, the TLI cost itself varies by less than 10 m/s over the L_2s family, so the variation in the total cost is due primarily to variations in the HOI cost, which varies by more than 140 m/s. The cost is minimized at the maximum amplitude halo, near a normalized position of $x = 1.1$ because

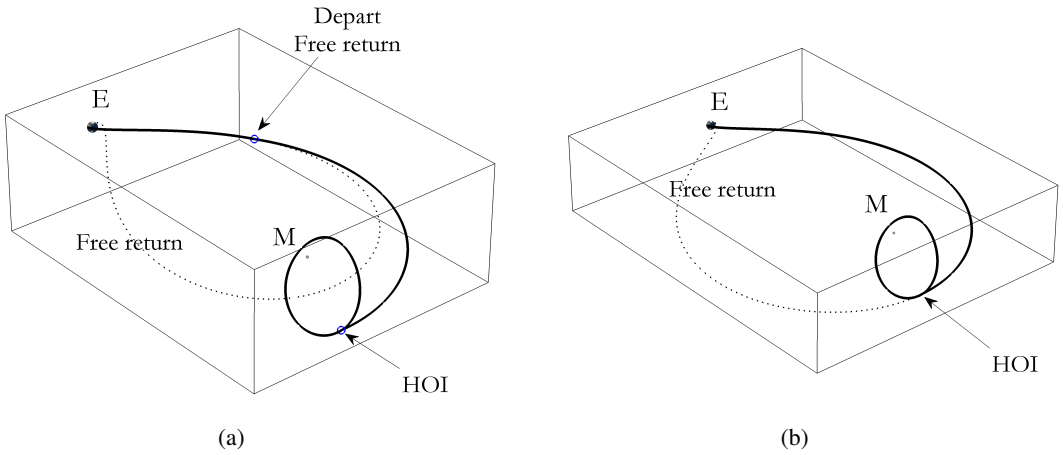

Figure 3. Example direct trajectories viewed in rotating-pulsating frame: a) free return flight time constrained and b) free return flight time unconstrained. The target halo is the same in each case.

the halo orbit velocity at insertion relative to the free return velocity is minimized at this point. Next, Figure 4(b) shows the free return's round trip flight time as a function of halo orbit location. As the halo orbit moves further from the moon, the flight time increases, starting at under 11 days at the near-rectilinear halo and climbing to over 12 days at the near-Lyapunov halo. Figure 4(c) shows that the geocentric inclination at TLI decreases as the halo's normalized x position increases. This is due to the fact that, in general, as the out-of-plane position of the free return at the moon increases, so does the declination of the free return's TLI velocity relative to the Earth-moon plane. Therefore, as the HOI point moves further out of the Earth-moon plane (as x decreases in the L_2s family), the higher the TLI inclination is expected to be. Figure 4(d) shows the atmospheric entry speed at Earth remains below 11.003 km/s for each case studied, which is acceptable under current heat shield capability.*

Table 2. Comparison of direct and LGA example cases.

Quantity	Direct 1	Direct 2	LGA 1	LGA 2	Units
Time on free return	1.0	6.0	0.0	1.0	day
Flight time to halo orbit	6.4	6.0	7.6	9.7	day
Round-trip free return flight time	10.0	11.7	-	12.8	day
Earth departure maneuver	3123	3135	3126	3128	m/s
Retargeting maneuver	99	0	-	23	m/s
Powered flyby maneuver	-	-	142	156	m/s
Orbit insertion maneuver	800	825	237	235	m/s
Total cost	4022	3960	3505	3542	m/s

Lunar Gravity Assist Results

A lunar flyby is performed en route to the halo orbit to save propellant. To achieve the proper approach trajectory for HOI, a propulsive maneuver is used at the flyby point. As with direct transfers,

*The maximum reentry speed during Apollo was 11.0685 km/s on Apollo 10.[20]

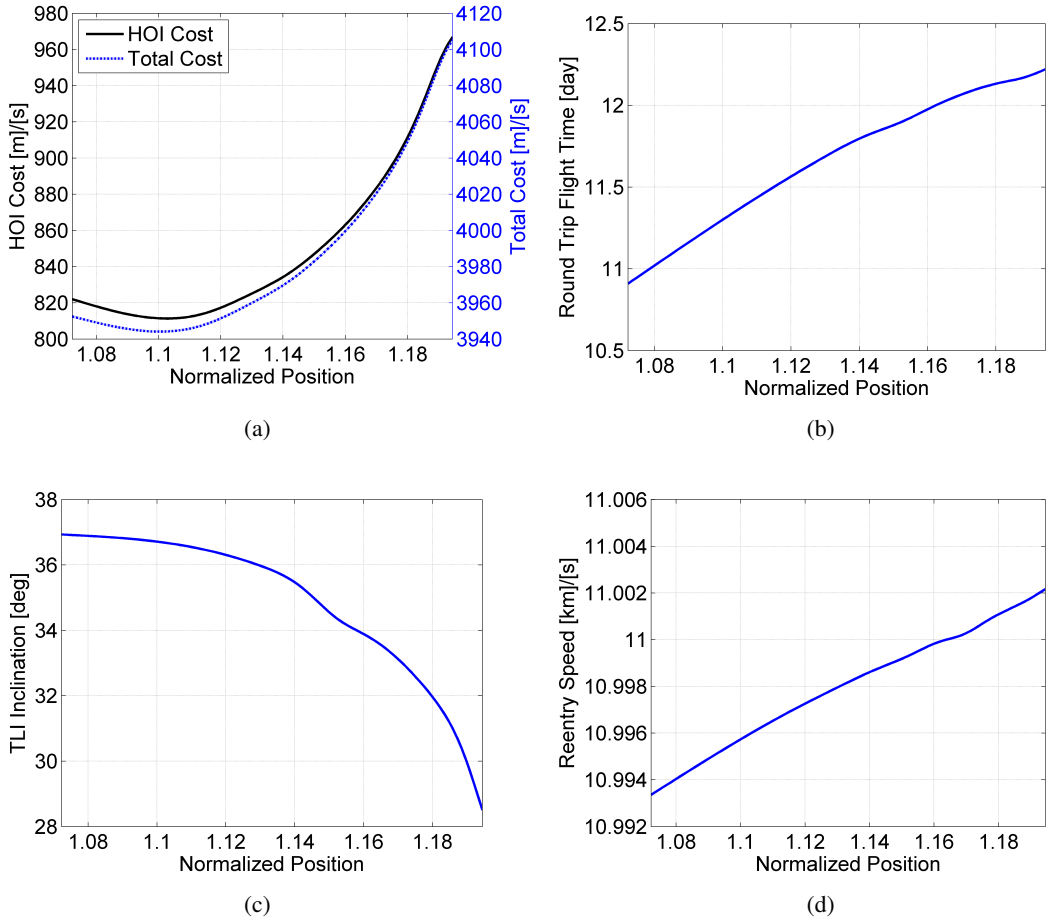

Figure 4. Direct transfers: a) total cost and HOI cost, b) round-trip free return flight time, c) TLI inclination, and d) reentry speed.

the spacecraft begins on a free return and departs it at a point to be determined by the optimizer. Because halos on the lunar farside are targeted, the flyby will often reside on the near side of the moon. This suggests that cislunar free returns should be used for LGA transfers. An example is shown in Figure 5 where the $x = 1.2991$ L_2s halo is targeted. Maneuver magnitudes are shown in Table 2 (labeled "LGA 2"). In this case, the spacecraft remains on the free return for one day, and the free return has a round-trip flight time of 12.8 days. Compared to the direct transfer, the LGA transfer requires four more days to reach the halo but costs nearly 420 m/s less. To understand the additional cost incurred by the free return requirement, a non-free return case is also optimized. The non-free return results are shown in Table 2 and labeled as "LGA 1". In this case, the outbound flight time has been reduced by over two days, and the ΔV requirement dropped by 37 m/s relative to the free return LGA example.

Free return LGA transfers are optimized for a range of halos spanning the L_2s family. For each target halo, the spacecraft's flight time on the free return is varied from 0.1 day to three days. Figure 6(a) shows the total cost, dominated again by the TLI maneuver. The near-Lyapunov halo is the least costly destination now, and the maximum amplitude halo is now the most expensive, which

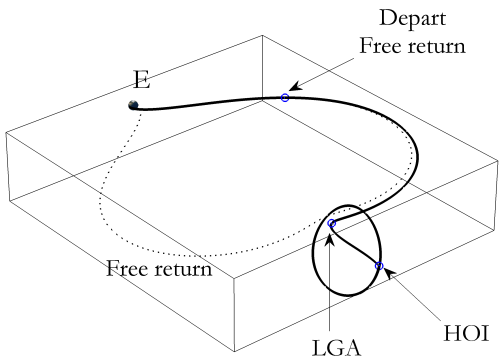

Figure 5. LGA transfer in Earth-moon rotating-pulsating frame.

is opposite the trend observed for direct transfers. For a given halo orbit, the cost increases with increased time spent on the free return. In Figure 6(b), the HOI cost is the sum of the retargeting, flyby, and orbit insertion maneuvers. The minimum HOI cost is 281 m/s at the $x = 1.19267$ halo with 0.1 day on the free return, and the maximum HOI cost is 431 m/s at the $x = 1.11364$ halo with three days on the free return. If the spacecraft is forced to remain on the free return for three days, the cost when targeting the near-Lyapunov halo increases to 314 m/s, which is less than the $x = 1.11364$ halo, even when the spacecraft is allowed to depart the free return after 0.1 day. Figures 6(c)–6(d) show the individual costs of the powered flyby and orbit insertion maneuvers. Figure 6(e) shows the flight time from Earth departure to orbit insertion at the target halo, and Figure 6(f) shows the round-trip free return flight time. In general, the outbound flight time increases when the spacecraft remains on the free return longer and when the halo orbit moves farther from the Earth. As the flight time on the free return increases from 0.1 day to three days, the outbound flight time to the near-Lyapunov halo increases from 10.4 days to 11.4 days. Because of the low cost of achieving the near-Lyapunov halo, it is an attractive destination for missions utilizing the outbound LGA. One possible concern, however, is that a spacecraft's view of the Earth will be temporarily blocked twice per each cycle of a near-Lyapunov halo. Choosing a halo with sufficiently large amplitude normal to the Earth-moon plane will eliminate this problem by providing a continuous line of sight to Earth.

ON-ORBIT ABORTS

The previous cases considered abort scenarios during the outbound phase of the mission. It is also necessary to consider aborts after the spacecraft has already inserted into the halo orbit. The halo orbit stay time and Earth return time are parametrically varied to study the magnitude of a single impulsive maneuver that transfers the spacecraft from the halo to a ballistic Earth return trajectory with specified EEI conditions. The analysis in this section does not consider LGA returns. It will be prudent to consider LGA returns in future research, however, because even though flybys may increase the return time in some cases, they may lower the cost of return in others and therefore may enable an abort when no direct return is possible.

Three L_2s halos are considered: a near-Lyapunov halo near L_2, a mid-range halo, and a near-rectilinear halo near the moon. The near-Lyapunov halo at $x = 1.1923$ with a maximum amplitude normal to the Earth-moon plane of 10000 km and a pseudo-period of approximately 14 days is shown in Figure 7(a) and Figure 7(b) where the elapsed time from orbit insertion is indicated in

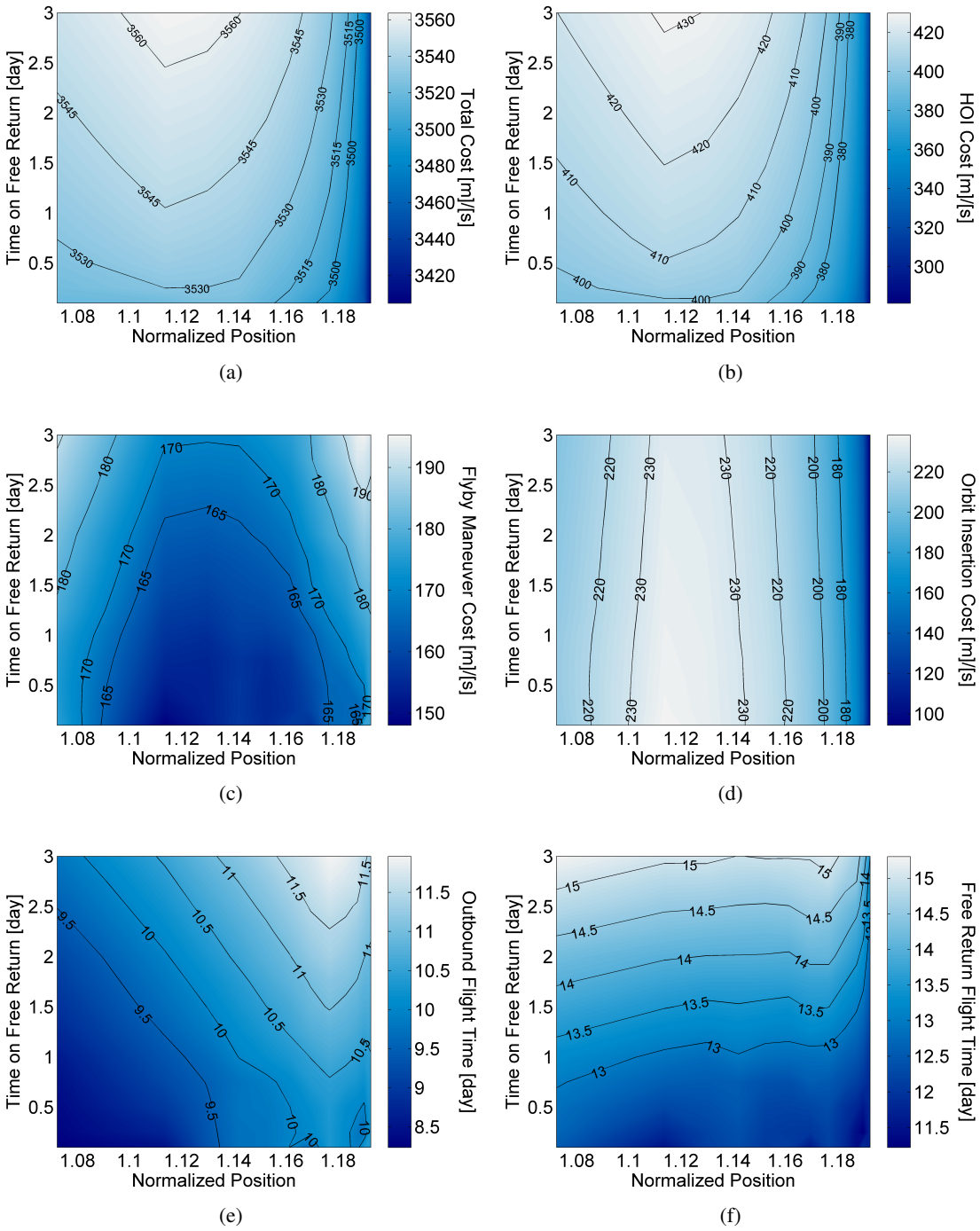

Figure 6. LGA transfers: a) total cost, b) total HOI cost, c) flyby maneuver magnitude, d) orbit insertion maneuver magnitude, e) TLI to orbit insertion flight time, and f) round-trip free return flight time.

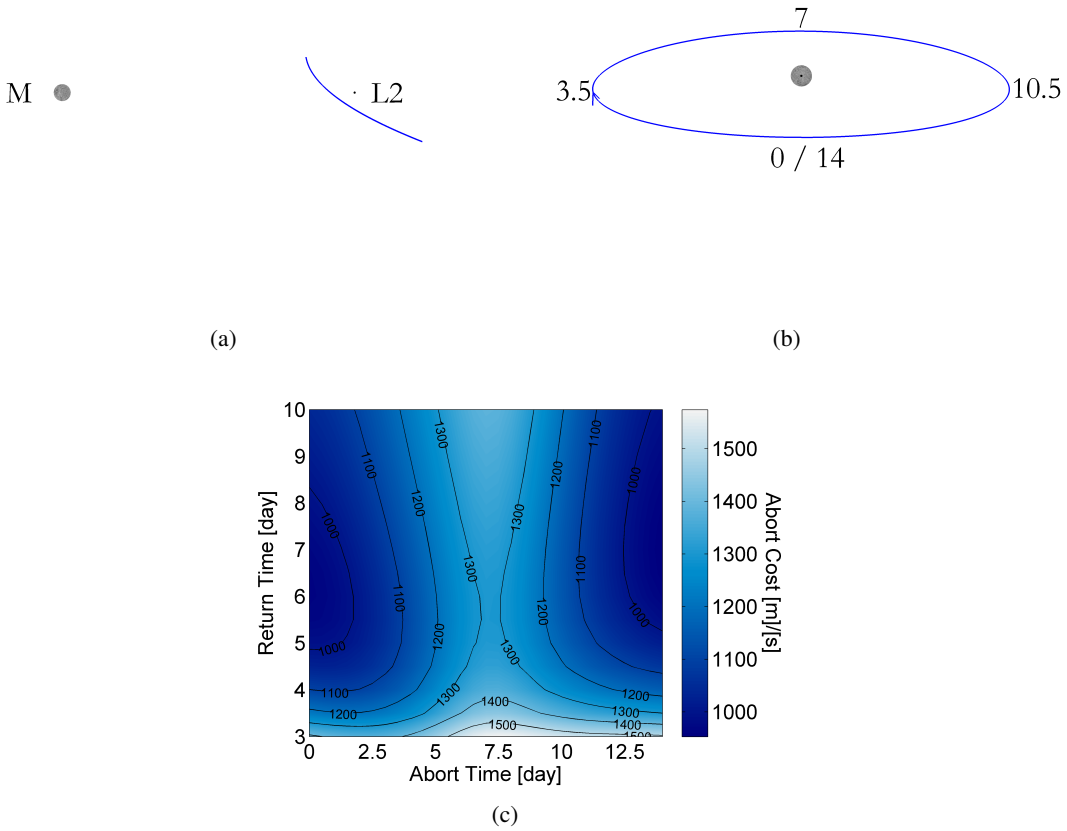

Figure 7. Near-Lyapunov halo on-orbit abort cost: a) halo projection in $\hat{x}\hat{z}$ plane of rotating-pulsating frame, b) view along moon-Earth line with approximate elapsed flight time labeled in days, and c) abort cost.

days. Figure 7(c) shows the optimal abort maneuver cost as a function of abort time and return time where the abort time is the elapsed time on the halo orbit and return time is the elapsed time from the abort maneuver to Earth return. For a given abort time, the abort cost is maximized when the return time is minimized, with some cases exceeding 1500 m/s at a return time of three days. For a given return time, the best time to abort is at the southern crossing of the vertical plane, which occurs near elapsed on-orbit flight times of zero and 14 days. The minimum cost of 953 m/s occurs at an abort time of 14 days with a return time of seven days; the maximum cost of 1580 m/s occurs at an abort time of 7.5 days with a return time of three days. The trends in abort cost do not perfectly repeat since the halo is pseudo-periodic. In addition to the abort cost rising as the return time decreases, another concern is the increased speed at EEI that may stress the spacecraft's thermal protection system. In no case for the near-Lyapunov halo did the Earth atmospheric entry velocity at an altitude of 121 km exceed 11.06 km/s.

Figure 8 shows a mid-range L_2s halo with a pseudo-period of about 13 days and its trends in abort cost. The minimum abort cost has decreased relative to the near-Lyapunov halo to 858 m/s at an abort time of zero days and a return time of six days. The maximum abort cost has increased to

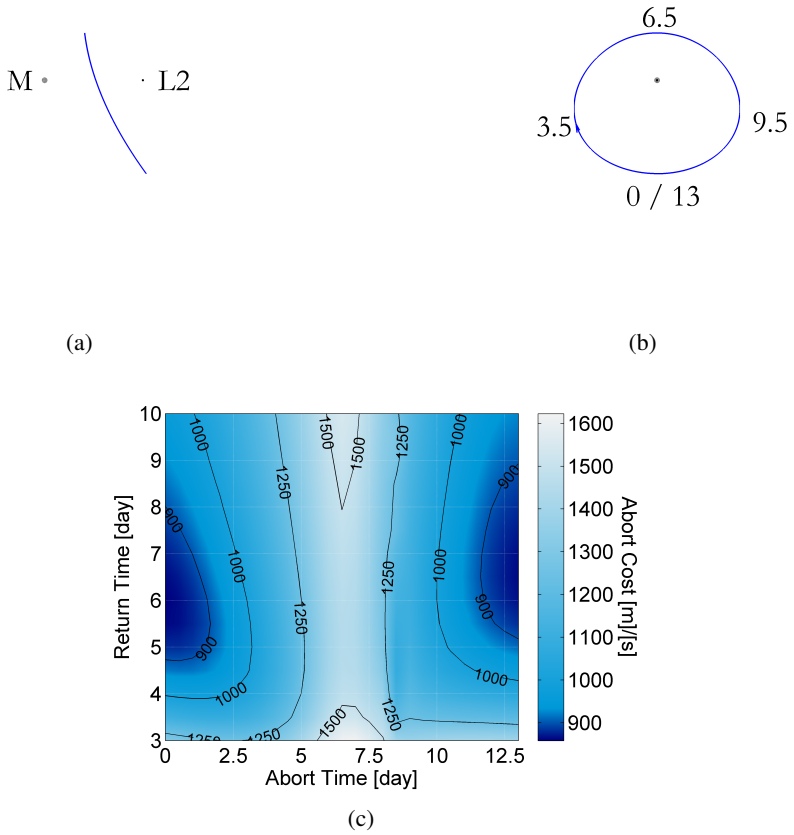

Figure 8. Mid-range halo on-orbit abort cost: a) halo projection in $\hat{x}\hat{z}$ plane of rotating-pulsating frame, b) view along moon-Earth line with approximate elapsed flight time labeled in days, and c) abort cost.

1624 m/s at an abort time of seven days and a return time of three days. The maximum EEI speed did not surpass 11.05 km/s. A near-rectilinear halo is shown in Figures 9(a)–9(b). The minimum abort cost in this case is 810 m/s and the maximum is 2034 m/s. Thus, over the three chosen halos, the minimum abort cost decreases as the halo approaches the moon from L_2, but the maximum abort cost increases.

ARCHITECTURE ANALYSIS

To understand what vehicle capabilities are required to perform the halo orbit mission with free return capability, various scenarios and architectures are analyzed for feasibility. The targeted halo orbit is the $x = 1.19267$ L_2s halo, which has a maximum amplitude normal to the Earth-moon plane of about 7500 km. This orbit was chosen because it maintains line-of-sight with Earth over its quasi-period and because, with an outbound LGA, it is one of the easiest halos to access. The outbound trajectory includes one day spent on a free return and may be either a direct or LGA transfer. The inbound transfer from the halo to Earth may also be a direct or LGA transfer. Hardware components for each mission include a launch vehicle (LV), an Earth departure stage (EDS), and

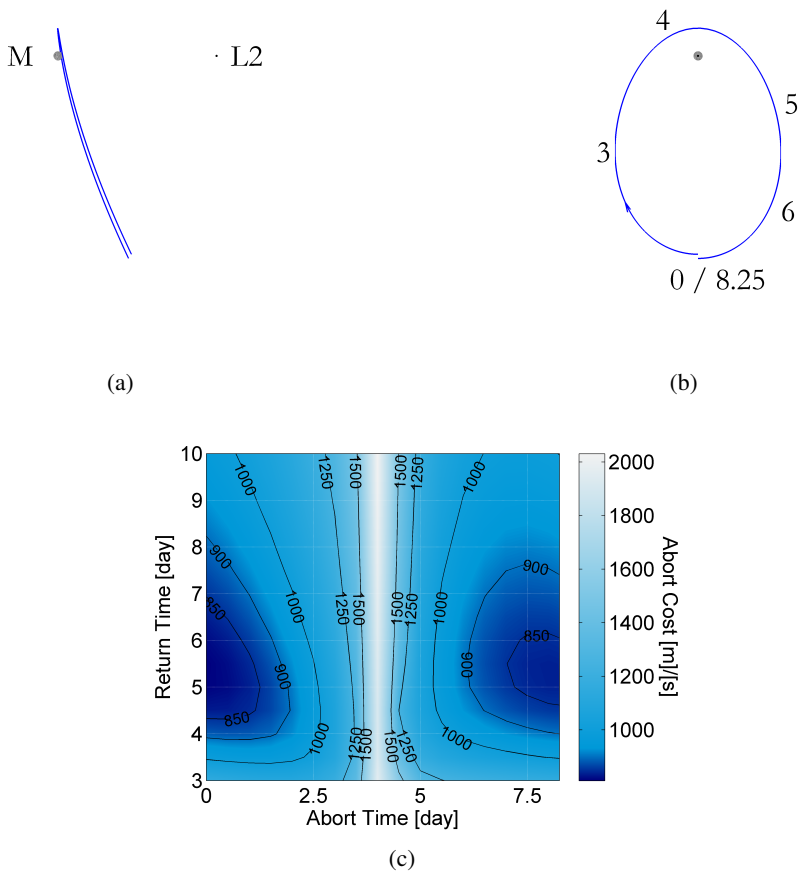

Figure 9. Near-rectilinear halo on-orbit abort cost: a) halo projection in $\hat{x}\hat{z}$ plane of rotating-pulsating frame, b) view along moon-Earth line with approximate elapsed flight time labeled in days, and c) abort cost.

a crew vehicle (CV), which is primarily responsible for HOI. Three heavy-lift LVs are considered, with LEO payload capabilities of 50000 kg, 75000 kg, and 100000 kg (Table 3). For comparison, other LVs are shown in Table 4. The three cryogenic EDSs considered have masses of 30000 kg, 45000 kg, and 50000 kg, each with a specific impulse of 460 s. Three CVs are considered with ΔV capabilities of 1000 m/s, 1500 m/s, and 2000 m/s. The orbital vehicle characteristics are listed in Tables 5–6. With two outbound and inbound transfer options, three LVs, three EDSs, and three CVs, 108 mission permutations are considered.

Table 3. Launch vehicle definitions.

Designation	Payload to LEO (kg)
1	50000
2	75000
3	100000

Table 4. Comparison launch vehicles.

Name	Status	Payload to LEO (kg)
Delta IV Heavy	Operational	22560*
Falcon Heavy	Proposed	53000†
SLS Block 1	Proposed	70000‡
SLS Block 1A	Proposed	105000‡
Saturn V	Retired	127000§

Table 5. Earth departure stage definitions.

Designation	Wet mass (kg)	Dry mass (kg)	Specific impulse (s)
1	30000	3000	460
2	45000	4500	460
3	50000	5000	460

Table 6. Crew vehicle definitions.

Designation	Wet mass (kg)	ΔV capability (m/s)
1	20000	1000
2	25000	1500
3	30000	2000

Tables 7–9 show the results of the architecture analysis. The sixth column in each table indicates the number of launches necessary to place the EDS and CV into the departure LEO. The seventh column indicates if the mission is feasible; if it is not, the next column lists the first hardware component whose capability does not meet its requirement for that mission. For EDS and CV failures, the margin of ΔV available is listed in the final column; for LV failures, the mass to LEO capability margin is listed.

With the 50000 kg LV, the only feasible single-launch mission is one with lunar flybys on both outbound and inbound legs. The outbound LGA flight time is 10.5 days with one day spent on the free return, and the inbound LGA flight time is 9.5 days. The use of two lunar flybys reduces the propulsive requirements but increases the transit time; this may be of concern depending on the longevity of crew life-support supplies. If a lunar flyby is used in combination with a direct transfer, the mission is feasible if EDS capability can be leveraged for HOI. One concern in this scenario is cryogenic boil-off over the translunar trajectory. No mission is feasible with EDS 1 and CV 2 or CV 3 unless CV propulsion can be leveraged for TLI; at least one LGA is required in each case. Upgrading to EDS 2 requires two launches but enables more feasible missions. Of particular interest, EDS 2 and CV 3 enable a direct-direct mission profile with an outbound flight time of 6.5 days and an inbound flight time of seven days. The use of two launches requires components to rendezvous in Earth orbit, and this may increase on-orbit flight time for crew. The 50000 kg LV cannot place EDS 3 into LEO. Table 8 presents the results for the 75000 kg LV configuration.

*Data available at `http://www.ulalaunch.com/site/docs/product_cards/DIV_product_card.pdf` [accessed 8 January 2013]

†Data available at `http://www.spacex.com/falcon_heavy.php` [accessed 8 January 2013]

‡Data available at `http://www.nasa.gov/pdf/623766main_8143_Singer-AD_industry_day-021312_FINAL3.pdf` [accessed 8 January 2013]

§Data available at `http://history.msfc.nasa.gov/saturn_apollo/documents/Introduction.pdf` [accessed 8 January 2013]

With EDS 1 and EDS 2, the on-orbit feasibility is identical to that of the 50000 kg LV. However, these missions now require only one launch. It is also feasible to utilize EDS 3 with the upgraded launch capability. With two launches, EDS 3, and CV 3, all outbound-inbound trajectory profiles are feasible. The 100000 kg LV (Table 9) enables every mission that is feasible with the 75000 kg LV to be accomplished with a single launch.

A direct-direct profile is advantageous because it has a shorter flight time and requires fewer maneuvers relative to profiles which contain LGAs and because it offers 100% outbound free return coverage. The main drawback of the direct-direct profile is that it is the most expensive mission in terms of ΔV. The only feasible direct-direct missions for the target halo require CV 3. With a 50000 kg LV, the EDS 2 and CV 3 combination enables a direct-direct mission with two launches. With a 75000 kg LV, the mission is feasible with EDS 2 or EDS 3, the latter requiring two launches. Both EDS 2 and EDS 3 combined with CV 3 enable a direct-direct mission after a single launch with the 100000 kg LV. Another drawback of the direct-direct profile is that because the direct outbound trajectory requires more propellant than the outbound LGA, less propulsive capability will remain for direct abort options once in the halo. As is evident from the above discussion of on-orbit orbits, there may be points during each pseudo-period where no direct abort is possible. The decision to use an outbound direct or LGA transfer may be decided by an analysis of mission risk. If it is determined that more risk is present on the translunar leg, a direct outbound profile is advantageous because it offers 100% free return coverage and requires fewer maneuvers than an LGA profile. However, if it is determined that adverse circumstances are more likely to arise while on-orbit in the halo, an outbound LGA is advantageous because it saves propellant for on-orbit aborts.

CONCLUSION

In this study, an overview of halo orbit and free return targeting has been presented, and outbound and inbound abort options for human missions to southern halo orbits about the translunar libration point have been analyzed. The use of a free return trajectory as a portion of the outbound transfer enables a period of propulsion-free Earth return capability. The added cost of the free return was found to be less than 10% of the nominal lunar gravity assist transfer cost, and for direct transfers the outbound free return did not differ significantly from the optimal non-free return transfer. The L_2s halo with maximum amplitude out of the Earth-moon plane was found to be the most costly destination for lunar gravity assist transfers but the cheapest destination for direct transfers in terms of the orbit insertion velocity impulse. On-orbit abort costs were computed for three L_2s halos: a near-rectilinear halo near the moon, a mid-range halo, and a near-Lyapunov halo near L_2. It was found that of the three, the near-rectilinear halo allowed the minimum abort cost at one point on its orbit but also required the maximum abort cost at another position on its orbit. The best abort time on each orbit occurs at the southern crossing, and the worst abort time occurs at the northern crossing. An architecture analysis was also performed to assess the requirements on launch and on-orbit vehicles for the halo orbit mission. Feasible scenarios were outlined for three classes of heavy-lift launch vehicles, Earth departure stages, and crew vehicles.

Halo orbits at L_2 provide an attractive destination for human missions for lunar farside exploration or as an aggregation orbit for other destinations in the Earth-moon system and beyond. L_2 halos also offer crewed missions a destination further from Earth than ever before to gain experience in long duration space flight while remaining within a few days flight time of Earth. The analysis in this study has shown the feasibility of using free returns as a method to mitigate risk from propulsion failure or other critical systems failures during the translunar portion of the mission. The analysis

Table 7. Architecture capabilities with 50000 kg launch vehicle capability to LEO.

Launch vehicle	Earth departure stage	Crew vehicle	Outbound	Inbound	Launches required	Feasible	First element failure	Failure element margin
1	1	1	Direct	Direct	1	No	CV	-48%
1	1	1	Direct	LGA	1	No*	CV	-18%
1	1	1	LGA	Direct	1	No*	CV	-20%
1	1	1	LGA	LGA	1	Yes		
1	1	2	Direct	Direct	2	No	EDS	-6%
1	1	2	Direct	LGA	2	No†	EDS	-6%
1	1	2	LGA	Direct	2	No†	EDS	-6%
1	1	2	LGA	LGA	2	No†	EDS	-6%
1	1	3	Direct	Direct	2	No	EDS	-17%
1	1	3	Direct	LGA	2	No†	EDS	-17%
1	1	3	LGA	Direct	2	No†	EDS	-16%
1	1	3	LGA	LGA	2	No†	EDS	-16%
1	2	1	Direct	Direct	2	No	CV	-48%
1	2	1	Direct	LGA	2	No*	CV	-18%
1	2	1	LGA	Direct	2	No*	CV	-20%
1	2	1	LGA	LGA	2	Yes		
1	2	2	Direct	Direct	2	No	CV	-22%
1	2	2	Direct	LGA	2	Yes		
1	2	2	LGA	Direct	2	Yes		
1	2	2	LGA	LGA	2	Yes		
1	2	3	Direct	Direct	2	Yes		
1	2	3	Direct	LGA	2	Yes		
1	2	3	LGA	Direct	2	Yes		
1	2	3	LGA	LGA	2	Yes		
1	3	1	Direct	Direct	—	No	LV	-17%
1	3	1	Direct	LGA	—	No	LV	-17%
1	3	1	LGA	Direct	—	No	LV	-17%
1	3	1	LGA	LGA	—	No	LV	-17%
1	3	2	Direct	Direct	—	No	LV	-17%
1	3	2	Direct	LGA	—	No	LV	-17%
1	3	2	LGA	Direct	—	No	LV	-17%
1	3	2	LGA	LGA	—	No	LV	-17%
1	3	3	Direct	Direct	—	No	LV	-17%
1	3	3	Direct	LGA	—	No	LV	-17%
1	3	3	LGA	Direct	—	No	LV	-17%
1	3	3	LGA	LGA	—	No	LV	-17%

* Feasible if EDS is leveraged for HOI.

† Feasible is CV is leveraged for TLI.

Table 8. Architecture capabilities with 75000 kg launch vehicle capability to LEO.

Launch vehicle	Earth departure stage	Crew vehicle	Outbound	Inbound	Launches required	Feasible	First element failure	Failure element margin
2	1	1	Direct	Direct	1	No	CV	-48%
2	1	1	Direct	LGA	1	No*	CV	-18%
2	1	1	LGA	Direct	1	No*	CV	-20%
2	1	1	LGA	LGA	1	Yes		
2	1	2	Direct	Direct	1	No	EDS	-6%
2	1	2	Direct	LGA	1	No†	EDS	-6%
2	1	2	LGA	Direct	1	No†	EDS	-6%
2	1	2	LGA	LGA	1	No†	EDS	-6%
2	1	3	Direct	Direct	1	No	EDS	-17%
2	1	3	Direct	LGA	1	No†	EDS	-17%
2	1	3	LGA	Direct	1	No†	EDS	-16%
2	1	3	LGA	LGA	1	No†	EDS	-16%
2	2	1	Direct	Direct	1	No	CV	-48%
2	2	1	Direct	LGA	1	No*	CV	-18%
2	2	1	LGA	Direct	1	No*	CV	-20%
2	2	1	LGA	LGA	1	Yes		
2	2	2	Direct	Direct	1	No	CV	-22%
2	2	2	Direct	LGA	1	Yes		
2	2	2	LGA	Direct	1	Yes		
2	2	2	LGA	LGA	1	Yes		
2	2	3	Direct	Direct	1	Yes		
2	2	3	Direct	LGA	1	Yes		
2	2	3	LGA	Direct	1	Yes		
2	2	3	LGA	LGA	1	Yes		
2	3	1	Direct	Direct	2	No	CV	-48%
2	3	1	Direct	LGA	2	No*	CV	-18%
2	3	1	LGA	Direct	2	No*	CV	-20%
2	3	1	LGA	LGA	2	Yes		
2	3	2	Direct	Direct	2	No	CV	-22%
2	3	2	Direct	LGA	2	Yes		
2	3	2	LGA	Direct	2	Yes		
2	3	2	LGA	LGA	2	Yes		
2	3	3	Direct	Direct	2	Yes		
2	3	3	Direct	LGA	2	Yes		
2	3	3	LGA	Direct	2	Yes		
2	3	3	LGA	LGA	2	Yes		

* Feasible if EDS is leveraged for HOI.

† Feasible is CV is leveraged for TLI.

Table 9. Architecture capabilities with 100000 kg launch vehicle capability to LEO.

Launch vehicle	Earth departure stage	Crew vehicle	Outbound	Inbound	Launches required	Feasible	First element failure	Failure element margin
3	1	1	Direct	Direct	1	No	CV	-48%
3	1	1	Direct	LGA	1	No*	CV	-18%
3	1	1	LGA	Direct	1	No*	CV	-20%
3	1	1	LGA	LGA	1	Yes		
3	1	2	Direct	Direct	1	No	EDS	-6%
3	1	2	Direct	LGA	1	No†	EDS	-6%
3	1	2	LGA	Direct	1	No†	EDS	-6%
3	1	2	LGA	LGA	1	No†	EDS	-6%
3	1	3	Direct	Direct	1	No	EDS	-17%
3	1	3	Direct	LGA	1	No†	EDS	-17%
3	1	3	LGA	Direct	1	No†	EDS	-16%
3	1	3	LGA	LGA	1	No†	EDS	-16%
3	2	1	Direct	Direct	1	No	CV	-48%
3	2	1	Direct	LGA	1	No*	CV	-18%
3	2	1	LGA	Direct	1	No*	CV	-20%
3	2	1	LGA	LGA	1	Yes		
3	2	2	Direct	Direct	1	No	CV	-22%
3	2	2	Direct	LGA	1	Yes		
3	2	2	LGA	Direct	1	Yes		
3	2	2	LGA	LGA	1	Yes		
3	2	3	Direct	Direct	1	Yes		
3	2	3	Direct	LGA	1	Yes		
3	2	3	LGA	Direct	1	Yes		
3	2	3	LGA	LGA	1	Yes		
3	3	1	Direct	Direct	1	No	CV	-48%
3	3	1	Direct	LGA	1	No*	CV	-18%
3	3	1	LGA	Direct	1	No*	CV	-20%
3	3	1	LGA	LGA	1	Yes		
3	3	2	Direct	Direct	1	No	CV	-22%
3	3	2	Direct	LGA	1	Yes		
3	3	2	LGA	Direct	1	Yes		
3	3	2	LGA	LGA	1	Yes		
3	3	3	Direct	Direct	1	Yes		
3	3	3	Direct	LGA	1	Yes		
3	3	3	LGA	Direct	1	Yes		
3	3	3	LGA	LGA	1	Yes		

* Feasible if EDS is leveraged for HOI.

† Feasible is CV is leveraged for TLI.

also demonstrated that various human halo mission permutations are feasible, even with the baseline heavy-lift launch vehicle, Earth departure stage, and crew vehicle. Future study into the minimum requirements for each of these elements would be useful in weighing the development costs of upgraded vehicles that enable more missions but may not be necessary to complete the baseline mission. The results of this research provide a preliminary mission designer the data necessary to understand the broad trajectory and architecture requirements for a human halo mission.

ACKNOWLEDGMENT

This research was carried out at Langley Research Center under a contract with the National Aeronautics and Space Administration. The author acknowledges the members of the Space Mission Analysis Branch for their discussions and feedback, especially Raymond Gabriel Merrill of NASA and David Cornelius of AMA.

REFERENCES

[1] N. R. Augustine *et al.*, "Seeking a Human Spaceflight Program Worthy of a Great Nation," Review of U.S. Human Spaceflight Plans Committee, Oct. 2009.

[2] R. W. Farquhar, "A Halo-Orbit Lunar Station," *Astronautics & Aeronautics*, Vol. 10, No. 6, 1972, pp. 59–63.

[3] R. W. Farquhar, "The Utilization of Halo Orbits in Advanced Lunar Operations," NASA TN D-6365, 1971.

[4] G. Gómez, K. Howell, J. Masdemont, and C. Simó, "Station-Keeping Strategies for Translunar Libration Point Orbits," *AAS/AIAA Space Flight Mechanics Meeting*, AAS Paper 98-168, Feb. 1998.

[5] R. G. Merrill, K. E. Goodliff, D. D. Mazanek, and J. D. Reeves, "Cis-Lunar Base Camp," *Global Space Exploration Conference*, GLEX Paper 2012.05.5.3x12703, May 2012.

[6] J. S. Parker, "Low-Energy Ballistic Transfers to Lunar Halo Orbits," *AAS/AIAA Astrodynamics Specialist Conference*, AAS Paper 09-443, Aug. 2009.

[7] J. S. Parker, "Monthly Variations of Low-Energy Ballistic Transfers to Lunar Halo Orbits," *AIAA/AAS Astrodynamics Specialist Conference*, AIAA Paper 2010-7963, Aug. 2010.

[8] R. K. Chen, E. M. Coombs, and J. J. Hibbert, "Lunar Farside Communications," Bellcomm TM-64-215-2, Nov. 1964.

[9] R. W. Farquhar, "The Flight of ISEE-3/ICE: Origins, Mission History, and a Legacy," *Journal of the Astronautical Sciences*, Vol. 49, No. 1, 2001, pp. 23–73.

[10] M. Jesick and C. Ocampo, "Ephemeris Model Optimization of Lunar Orbit Insertion from a Free Return Trajectory," *AAS/AIAA Astrodynamics Specialist Conference*, AAS Paper 11-452, Aug. 2011.

[11] C. A. Ocampo, "An Architecture for a Generalized Spacecraft Trajectory Design and Optimization System," *International Conference on Libration Point Missions and Applications*, June 2002.

[12] C. A. Ocampo, "Finite Burn Maneuver Modeling for a Generalized Spacecraft Trajectory Design and Optimization System," *Annals of the New York Academy of Sciences*, Vol. 1017, No. 1, 2004, pp. 210–233.

[13] W. M. Folkner, J. G. Williams, and D. H. Boggs, "The Planetary and Lunar Ephemeris DE 421," IPN Progress Report 42-178, Aug. 2009.

[14] C. H. Acton, "Ancillary Data Services of NASA's Navigation and Ancillary Information Facility," *Planetary and Space Science*, Vol. 44, No. 1, 1996, pp. 65–70.

[15] K. C. Howell, "Three-Dimensional, Periodic, 'Halo' Orbits," *Celestial Mechanics and Dynamical Astronomy*, Vol. 32, No. 1, 1984, pp. 53–71.

[16] R. W. Farquhar and A. A. Kamel, "Quasi-Periodic Orbits About the Translunar Libration Point," *Celestial Mechanics and Dynamical Astronomy*, Vol. 7, No. 4, 1973, pp. 458–473.

[17] J. V. Breakwell and J. V. Brown, "The Halo Family of 3-dimensional Periodic Orbits in the Earth-Moon Restricted 3-body Problem," *Celestial Mechanics and Dynamical Astronomy*, Vol. 20, No. 4, 1979, pp. 389–404.

[18] K. C. Howell, "Families of Orbits in the Vicinity of the Collinear Libration Points," *Journal of the Astronautical Sciences*, Vol. 49, No. 1, 2001, pp. 107–126.

[19] M. Jesick and C. Ocampo, "Automated Generation of Symmetric Lunar Free Return Trajectories," *Journal of Guidance, Control, and Dynamics*, Vol. 34, No. 1, 2011, pp. 98–106.

[20] R. W. Orloff, *Apollo by the Numbers: A Statistical Reference*, pp. 291,305. Washington: U. S. Government Printing Office, 2000.